Study and Characterization of Composites Materials Based on Polypropylene Loaded with Olive Husk Flour

Boukerrou Amar,[1] Krim Salem,[1] Djidjelli Hocine,[1] Ihamouchen Chadia,[1] Martinez J. Juan[2]

[1]*Laboratoire des matériaux organiques, Département de Génie des Procédés, Université Abderrahmane MIRA, Route de Targa-Ouzemmour, Béjaïa 06000, Algeria*
[2]*Laboratoire de Génie électrique, (UMR-CNRS 5003) Université Paul Sabatier, Toulouse, France*

Received 18 November 2009; accepted 31 December 2010
DOI 10.1002/app.34084
Published online 23 May 2011 in Wiley Online Library (wileyonlinelibrary.com).

ABSTRACT: In Algeria, a significant quantities of olive husk are rejected to nature causing by the way major nuisances to environment, to give us a reason for which our work is focused on the valorization of this waste by its incorporation in a polypropylene matrix. The hydrophilic nature of natural fibers affects negatively its adhesion to hydrophobic polymeric matrix. To improve interfacial adhesion, two modes of chemical treatments were done using vinyltriacetoxysilane (VTAS) and maleic-anhydride-polypropylene (PPMA) compatibilisant agent. Several formulations of PP filled with 10 and 20% by mass of olive husk flour treated (OHFT) and untreated (OHFUT) were prepared. The chemical modification of olive husk flour was studied by Fourier transform infrared (FTIR) spectroscopy. The tensile properties, the water-absorption behavior, the thermal degradation properties, and crystallinity of the composites were investigated. It was found that, the incorporation of the treated and untreated OHF improves the thermal stability of the composites. However, the use of the compatibilizer agent PPMA leads to a better thermal stability compared with the treatment of the OHF by the VTAS and the OHFUT. © 2011 Wiley Periodicals, Inc. J Appl Polym Sci 122: 1382–1394, 2011

Key words: composites; compatibilization, poly (propylene); thermal properties; olive husk flour

INTRODUCTION

Polypropylene as one of the most popular versatile thermoplastic polymers, provides many advantages with regard to its low cost, recyclability, and high thermal stability, and has yielded many kinds of composites.[1]

The search for new materials takes a significant place in the history of technology. The industrialists use more and more composite materials with fibers reinforcement. In particular, they have searched to conceive, to develop and to characterize new materials intended to be used in sectors of high technology such as aeronautics and the military field and in daily fields like for automotive applications, the leisures, and the habitat. The objectives of research on new materials are: to profit of performances, to low manufacturing cost of the products, and to save or even to improve the reliability of finished products. Moreover, in a preoccupation of environmental protection and public health, the composites tend to integrate an ecological character (ex: recycled or biodegradable matters).[2] A considerable attention has been picked up to use the natural fibers both in the literature and in industry in recent years. Advantages of natural fibers over conventional reinforcement such as glass or carbon fibers are the low cost and low density, biodegradability, as well as high specific properties.[3]

The main drawbacks of such composites are their water sensitivity and relatively poor dimensional stability, poor adhesion to basically all matrix polymers, as well as poor processability and esthetics at high wood contents. Although drawbacks are outweighed by the advantages in most cases and these composites are used in huge quantities, the optimization of component properties, structure and interfacial interactions may lead to even more advantageous solutions.[4–6]

Several studies showed that fiber-polymer bonding can be improved by the use of coupling agents. In some cases, it was verified that the use of coupling agents also served to moderate and somewhat mitigate moisture movement through the composite, thus improving the mechanical properties of the materials.[7,8]

Chemical or physical modifications are usually applied to improve the interfacial adhesion of the composites, and dimensional stability. The use of coupling agent, such as alkali treatments, acetylation, graft copolymerization, or the use of maleic-anhydride-polypropylene (PPMA) has been reported to overcome the incompatible surface polarities

Correspondence to: Krim Salem (krim_salem@yahoo.fr).

© 2011 Wiley Periodicals, Inc.

between the natural fiber and polymer matrix.[9] Olive husk, one of several lignocellulosic materials, is an agricultural industrial residue produced as by-products during the olive milling process in olive-producing countries such as Algeria.[10] The Algerian olive oil industry produces about 200,000 tons of solid wastes and this quantity tends to increase every year. It is possible to recover 15–22 kg olive oil and 35–45 kg olive residue from 100 kg of olive.[11,12] On the other hand, there are only a few work reported in the literature on olive husk rejects and their uses in many applications involving mainly the production of thermal energy, fertilizer as well as food for animals.[13] Unfortunately, in our country large quantities of this waste which is released into the wild or outright incinerated causing major inconvenience for the environment. For this reason, this study aims both to enhance the olive husk by it incorporating into a PP matrix. Second, the objective of this work was to investigate the modification of interfacial adhesion forces between olive husk flour (OHF) and PP matrix to increase their compatibility by two different methods.

The first method was based on the chemical treatment of OHF through silanization by reacting the hydroxyl groups of the cellulose material with silanol groups of the vinyltriacetoxysilane (VTAS), whereas the second one consisted of using a coupling agent PPMA to improve the interfacial bonding between the OHF and the PP matrix. The various composite materials obtained were studied by different analytical techniques as: FTIR spectroscopy, x-ray diffraction, tensile properties, and water-absorption capacity.

EXPERIMENTAL

Materials

OHF (<100 μm) from Béjaïa, Algeria, was used as filler. It was previously dried in an oven at 80°C until its weight reached a constant. Isotactic polypropylene [melt flow index (230°C/2,16 kg): 3 g/10 min] was provided by ALL PLAST (Akbou-Béjaïa, Algeria). Maleic anhydride (MA, 99.5%), vinyltriacetoxysilane (VTAS, 95%) from SIGM-ALDRICH Chimie Gmbh, Germany, and peroxide benzoyl.

Synthesis of the coupling agent (PPMA)

According to the procedure reported previously by J. M. Garcia Martinez.[14] The grafted polypropylene (PP) was synthesized in a solution state. In typical solution-grafting process, 10 g of PP and 25% (w/w) of anhydride maleic were dissolved in 100 mL xylene at 140°C under a nitrogen atmosphere and continuous stirring. After complete dissolution of PP, 0.3% (w/w) of free radical initiator PBO (benzoyl peroxide) was added. The reaction was allowed to proceed at 3 h. The graft polymer solution was precipitated by adding acetone at room temperature. After thoroughly washing with acetone, the graft polymer was transferred to an oven at 80°C for 24 h to remove any trace of residual solvent and maleic anhydrid.

Fiber surface treatment

OHF (<100 μm) was added into a mixture of methanol/water (90/10, w/w) and stirred for 12 h at room temperature to clean the fibers by removing starch and waxes from the surface. The flour was then filtered and dried in an oven at 80°C for 12 h. For the flour surface treatment, 5 wt % silane was dissolved in a methanol/water mixture at room temperature and the pH of the solution adjusted to four with the addition of acetic acid, according to the procedure reported previously by C. Nah and al.[15] Silanes are more stable if they are applied from a slightly acid solution. After the continuous stirring of the solution for 10 min, the dried OHF was immersed in the solution and stirred for 24 h at room temperature. The OHF was then filtered and dried at 80°C for 12 h.

Preparation of the composites

Before to mixing, the OHF was dried in a drying oven for 6 h at 80°C. PP/OHF composites were prepared by the process of injection molding, at 190°C and 115 rpm, the residence time was 2 min. The extrudates were cooled and crushed to be used thereafter in the compression molding. The formulations based on mixing PP with the OHF before and after chemical treatment and also in the presence of the PPMA compatibilizer according to Table I. Sheets of about 1-mm thickness were obtained by compression molding (Zwick/Roell) at 190°C, under a stress of 300 kN for 5 min, followed by cooling. Teflon films were used to avoid the adhesion of PP to the stainless surface of the mold. Standard (ISO 527, juin 1993, Type HII) specimens were cut from the pressured sheets for tensile measurements.

Techniques

Fourier transform infrared spectroscopy

The method used to evaluate the chemical modification is Fourier transform infrared (FTIR) spectroscopy. The FTIR spectra of the nonmodified and modified OHF and also for the virgin PP and PPMA were obtained to detect the new absorption bands depicted in the chemical modification. The FTIR was performed using a FTIR SHIMADZU FTIR-8400S

TABLE I
Formulation Codes of PP/OHF Composites Used

Components	Formulations						
	F0	F10N	F10S	F10P	F20N	F20S	F20P
PP (wt %)	100	90	90	85	80	80	75
Untreated OHF (wt %)	0	10	0	10	20	0	20
Treated OHF (wt %)	0	0	10	0	0	20	0
PPMA (wt %)	0	0	0	5	0	0	5

Spectrometer. The spectrometer was used in the absorbance mode with a resolution of 4 cm^{-1} in the range of 400–4000 cm^{-1}. The samples were analyzed using the KBr pellet method.

X-ray analysis

Wide-angle X-ray scattering (WAXS) analysis used in general to determine the mineralogical composition of a sample. This method is applicable only to crystalline mediums. The analyses of diffraction of x-rays were carried out on an apparatus of the type X PERT Pro Panalytical, using the Cu-Kα1 radiation (λ = 1,540,598 E). The scans were performed within the range of $2\theta = 2°$–$70°$ with the scanning step of 0.01° in the reflection geometry.

Tensile test

The strength of the OHF reinforced PP composites was determined using a tensile testing machine of the type "Zwick/Roell," Tests were carried out according to the standard "ISO 527, June 1993" at the ambient temperature, Six measurements were conducted for each sample, and the results were averaged to obtain a mean value.

Rheological properties: melt flow index

The melt flow index (MFI) was given by means of a plastometer of extrusion. MFI of OHF/PP composites was measured according the standard: ISO 1133 ASTM D 1238 using a load of 2.16 kg at 230°C. Five measurements were conducted for each sample, and the results were averaged to obtain a mean value. After weighing, the water absorption (WA) of the samples was calculated as eq. (1).

$$\mathrm{MFI} = 600 * \frac{\text{weight of extudates}}{\text{time of flow}} \left(\mathrm{g/10min}\right) \quad (1)$$

Water-absorption tests

Water absorption of composite was examined by immersion of sheet sample of 1-mm thickness in distilled water at room temperature for 146 h, periodically measuring the increase in weight of the sample. After weighing, the WA of the samples was calculated as eq. (2).

$$\mathrm{WA}(\%) = W_2 - W_1/W_1 \times 100 \quad (2)$$

where W_1 and W_2 are the weights of the sample before and after immersion in distilled water, respectively.

Thermogravimetric analysis

Thermogravimetric analysis (TGA) was used to investigate thermal decomposition behavior of OHF/PP composites. The thermograms of the various samples were recorded using a thermogravimetric apparatus of type SETARAM TGA 92, controlled by a microcomputer. Tests were done under nitrogen at a scan rate of 10°C/min in a programmed temperature range of 20–700°C. A sample was used for each run. The weight change was recorded as a function of temperature. Derivative peak temperature (DTG) was taken as the maximum temperature acquired from the differentiation of the weight change as a function of time.

Scanning electron microscopy

Scanning electron microscopy (SEM) was used to monitor, the fracture surface of the composites after frozen the samples in liquid nitrogen. SEM analysis was performed using a FEI CONTA 200.

RESULTS AND DISCUSSION

Characterization of the components

Characterization of OHF untreated and treated with a VTAS

FTIR analysis of the OHF before and after treatment with VTAS. The FTIR spectra of the OHF untreated and treated by the VTAS are shown in Figure 1, The strong absorption between 3400 and 3600 cm^{-1} in all FTIR spectra is caused by the (OH) groups, as hydroxyl substitution is not high enough and these bands are always present. However, it is clear from the spectra of OHFs treated that there is a reduction

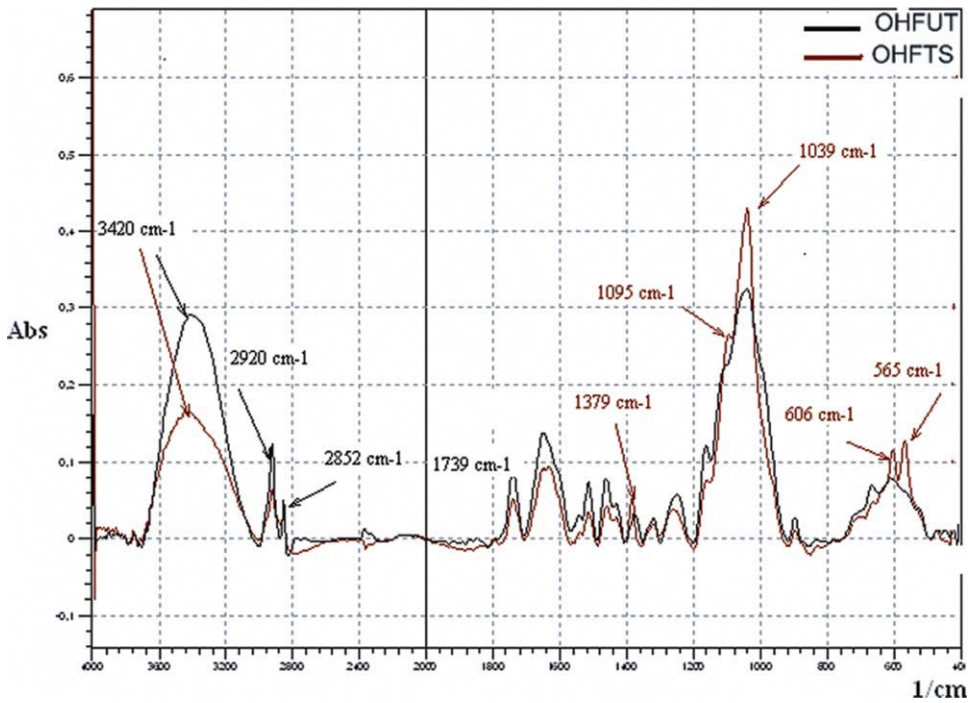

Figure 1 FTIR spectra of the OHF untreated and treated. [Color figure can be viewed in the online issue, which is available at wileyonlinelibrary.com].

of this bond as a result of silanization. We also observe, on the two spectra the presence of an absorption band in the vicinity of 1740 cm^{-1} characteristic with the stretching vibrations of carbonyls corresponding to the acetyl groups, aldehyde, carbonyl, and ester contained in the structure of hemicellulose, lignin and the extractable. In addition, we also note a broad absorption band in the rounding from 950 to 1195 cm^{-1} attributed to the asymmetrical stretching vibrations of the bonds Si—O—Si and Si—O—CH3, the presence of these connections is a result of the reaction of condensation between the silanols and hydroxyls of the OHF which leads to the formation of connections (Si—O—C). In addition, the other groupings of silanol are able to form hydrogen bridges where the condensation with another silanol to form connections (Si—O—Si), detected by FTIR. These are corroborated with the results of Demir, Boufi, and Wang.[16–18] We also observe an absorption band in the region of 1625 cm^{-1} attributed to connection (C=C) of the vinyl groups of the coupling agent. FTIR analysis confirms that the reaction of silanization took place, which makes it possible is to propose a suitable reactional mechanism for this modification (See Scheme 1).

Thermogravimetric analysis of OHF. The thermal stability of both untreated and treated OHF was studied by TGA under nitrogen atmosphere in the range 20–800°C at a heating rate of 10°C/min.

Thermal behavior of the OHF untreated and treated with the VTAS is shown in Figure 2. Both TGA curves indicate the same thermal behavior of the OHF untreated and treated. We can observe that the OHF untreated (OHFUT) begins to degrade at 210°C but the OHF treated (OHFT) with a VTAS begins to degrade at 201°C, this reduction in the initial temperature of decomposition can be attributed to the elimination of some hydrogen bonds which requires significant energy to destroy them.

The different steps from degradation of the OHF are given as following:

The first peak appeared on thermograms DTG is in the rounding of 100°C which is attributed to the evaporation of water.

The second peak is localized at 260°C for the OHFUT and at 250°C for the OHFTS, this zone of degradation corresponds to the temperature of decomposition of hemicellulose and the glycedic bonds of cellulose. These results are in agreement with the results of Pracella and Mader.[19,20]

The third peak is recorded at 325°C, it corresponds to the decomposition of cellulose. At 350°C, we can observe a fourth peak, it is probably assigned to the decomposition of lignin, These results are in perfect agreement with those obtained by Mader andLi .[20,21]

Characterization of PP and the PPMA

FTIR analysis of the PP and the PPMA

The FTIR spectra of the OHF untreated and treated by the VTAS are shown in Figure 3. We can be

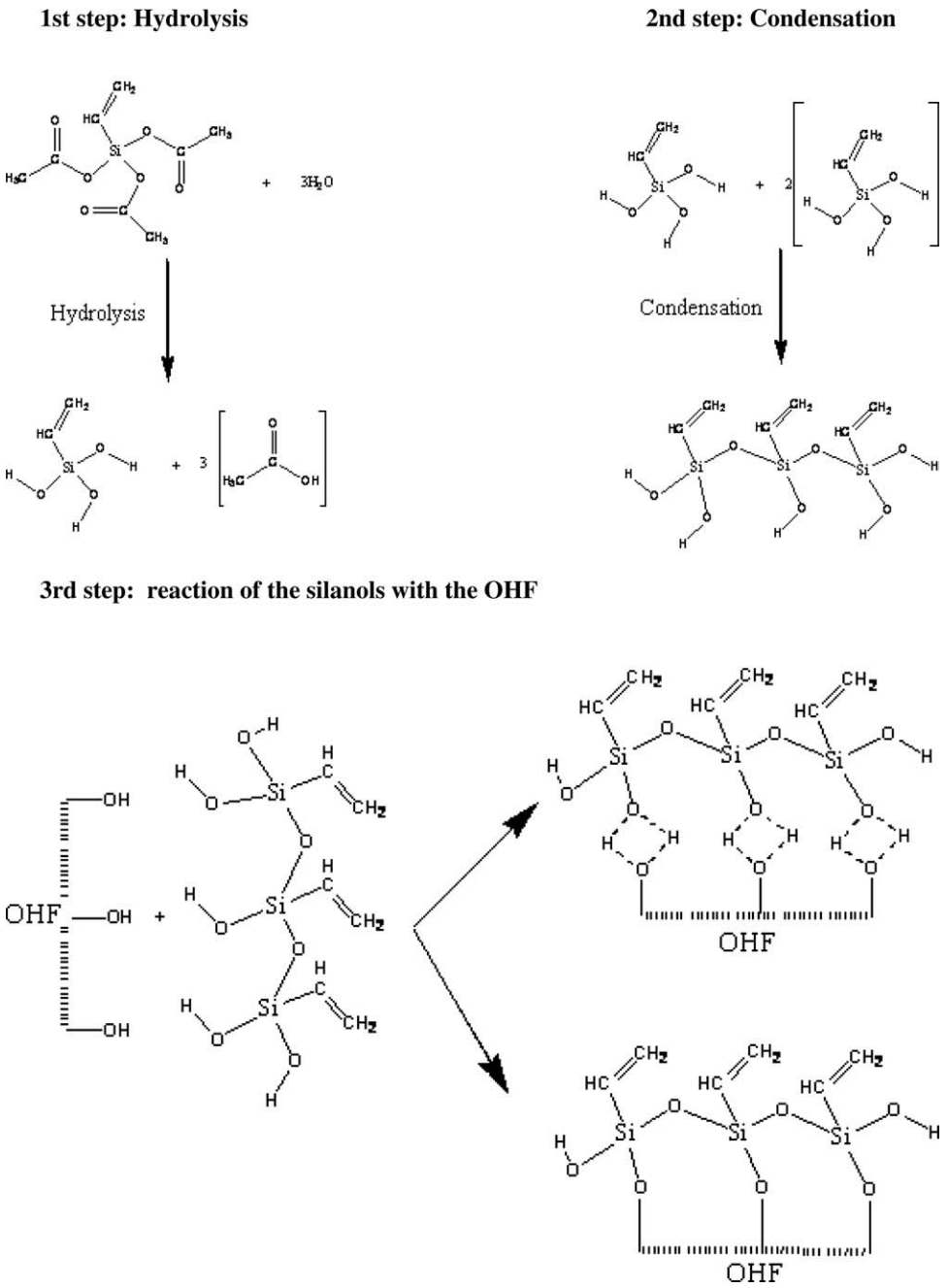

Scheme 1 Mechanism between the olive husk flour and the vinyltriacetoxysilane.

observed that for both spectra FTIR presented in Figure 3, the composition of the PP and the PPMA is the same in all the broad bands (400–4000 cm^{-1}). The only difference observed between the spectra is localized in the broad bands around 2000 and 1600 cm^{-1}, indeed, the appearance of bands at around 1785 and 1708 cm^{-1} on the spectrum of the PPMA correspondent to the symmetrical stretching vibrations of carbonyls (C=O). What is not observed on the spectrum of the PP, all these information confirm that the presence of the MA groups in the molecular structure of the PP modified. These results are in perfect agreement with those obtained by Kim.[22] Moreover, the absence of the characteristic band of the double bonds (C=C) which is generally localized at 1600 and 1500 cm^{-1} is a signature of the effectiveness of washing with acetone to remove the MA not reacted. So, we can propose the reactional mechanism of grafting the MA on the PP as following (See Scheme 2):

Thermogravimetric analysis of the PP and the PPMA

From Figure 4, which displays the results of TGA of the virgin PP and PPMA, it can be seen that the

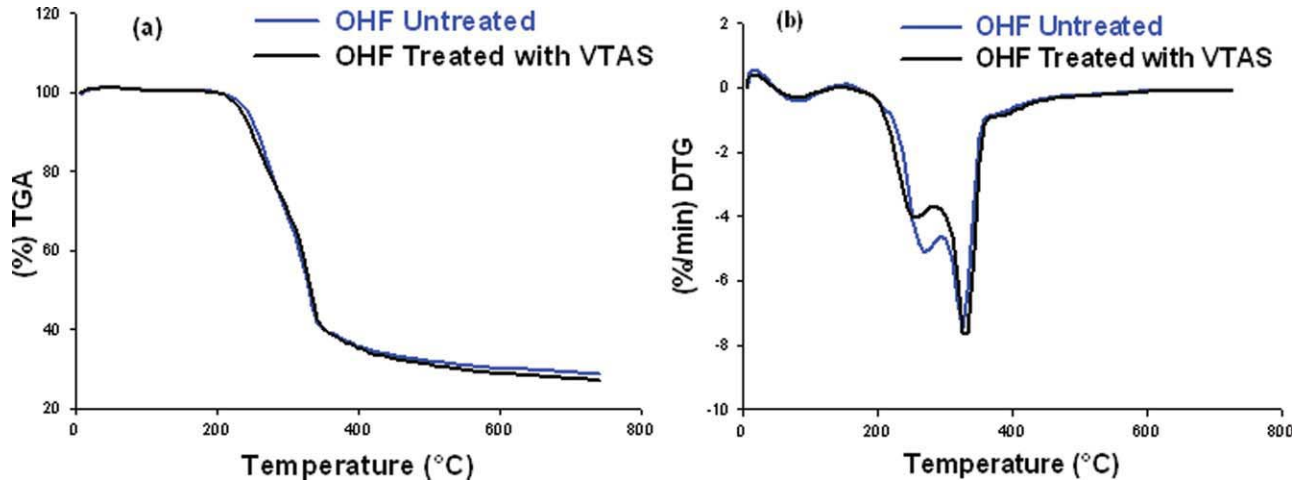

Figure 2 TGA–DTA thermograms of OHF treated and untreated. (a) TGA curves, (b) DTG curves. [Color figure can be viewed in the online issue, which is available at wileyonlinelibrary.com].

curves for PPMA a lower loss mass it observed around 110°C which is probably due to the water evaporation. This quantity of water was evaluated starting from the results obtained by the TGA and gives a value of about 3%. This quantity of water is due to the presence of the anhydrides groups which are polar and consequently they present an affinity with water. In addition, the presence of the AM on the PP induced to a slight reduction in the beginning of the decomposition compared with a virgin PP it is from 397°C for the virgin PP and 381°C for PPMA. Furthermore, the thermal degradation is pronounced, the loss of mass at evaluated in background: 97 and 94% for the virgin PP and PPMA, respectively. In the slight of these results, we can conclude that the grafting reaction of MA on the PP, generates a slight loss of thermal stability which is evaluated at 16°C. According to the thermograms TGA, we notice that the quantity of ashes is very weak and they are formed starting from 450°C, and according to Turmanova,[23] this result is attributed to the evaporation low-weight molecules generated by the depolymerization of polypropylene during its thermal degradation. The mechanism of the thermal degradation according to Scheme 3:

Characterization of the composites

X-ray diffraction studies

The curves of x-rays diffraction (XRD) of matrix PP and the composites are represented in Figure 5. According to Kim, Lin, and Jiang,[22–25] confirmed that the polypropylene has four crystallographic forms: α-form, β-form, γ-form and the smectite form. Indeed, we can notice these peaks on the curves of x-rays diffraction of our composites. The α-form can be found at the scattering angles 2θ of α1: 14.1°, (110) α2: 16.9°, (040) α3 : 18.5° (130), and α4: [21.3° (111) and 21.8° (131)]. The x-rays diffraction spectrum of the PP/OHF shown in Figure 5 shows a predominant α-form. Some traceable amounts of the β-form [β_1: 16.1° (300) and β_2: 23.1° (221)] can also be found in the PP/OHF. The absences of the γ-form and the smectic form are expected since the γ-form can only be found by crystallization under very high pressure and the smectic form is generated under extremely fast cooling conditions.

The treatment of these spectra of x-rays diffraction, we made it possible to determine the rate of crystallinity of the various worked out composites, the whole of the results are summarized in the Table II. The evolution of the rate of crystallinity according to the rate of the treated and untreated OHF, we can notice that the rate of crystallinity decreases as the rate of the OHF increase. It can be explained by the increase in the proportion of the amorphous phase in the OHF. In other words, the OHF used in this study has a significant proportion in hemicellulose and the lignin which are presented at the amorphous state in the OHF. Moreover, we can also

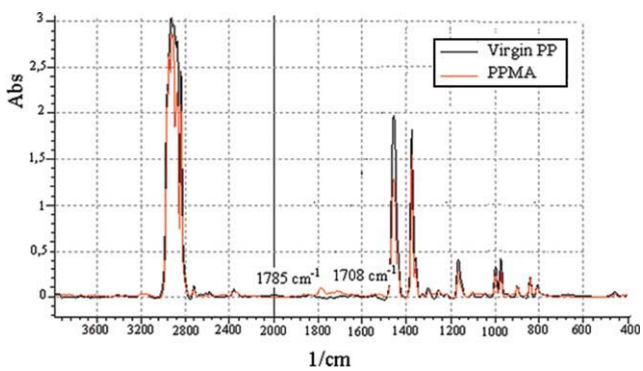

Figure 3 FTIR spectra of the PP and the PPMA. [Color figure can be viewed in the online issue, which is available at wileyonlinelibrary.com].

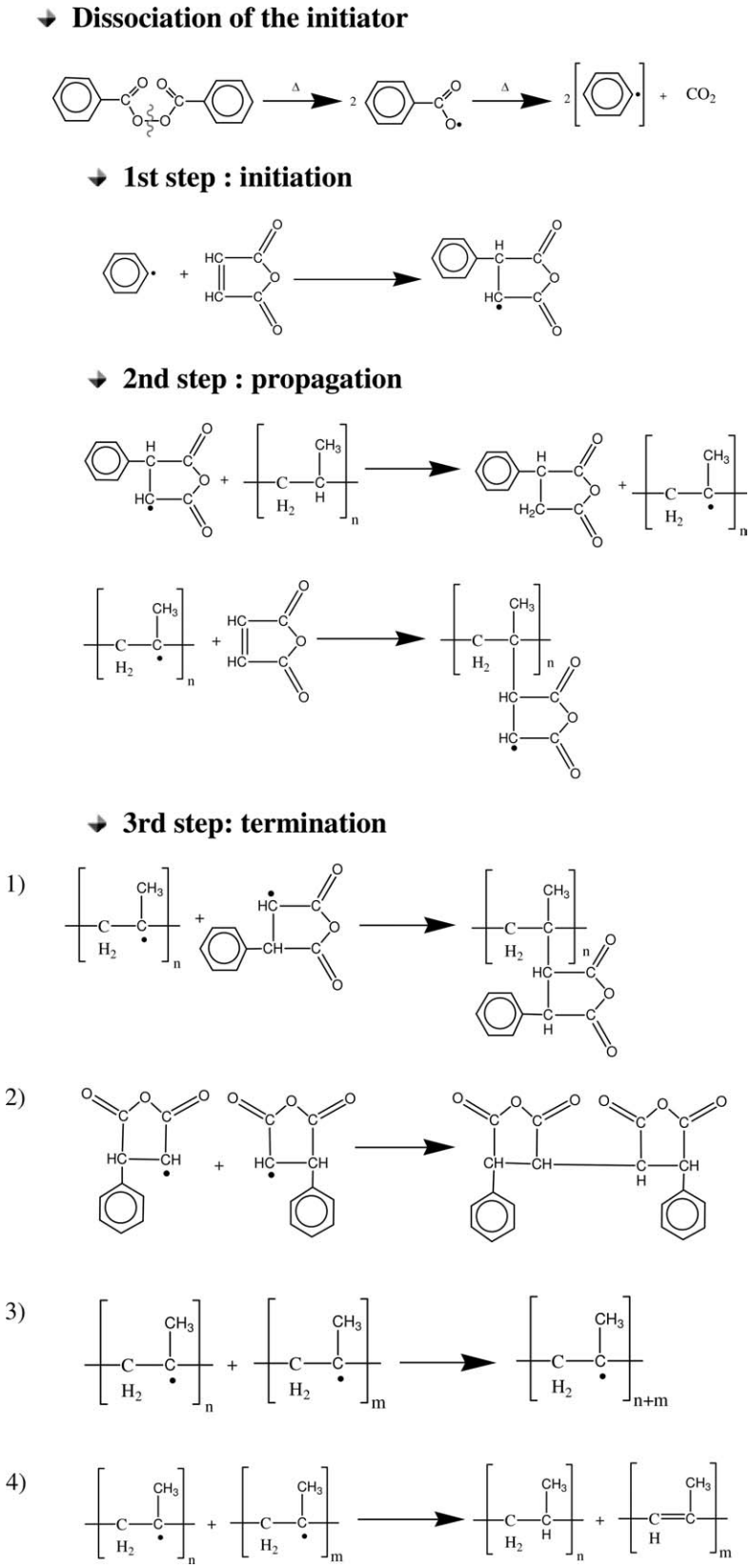

Scheme 2 Mechanism of grafting the MA on the PP.

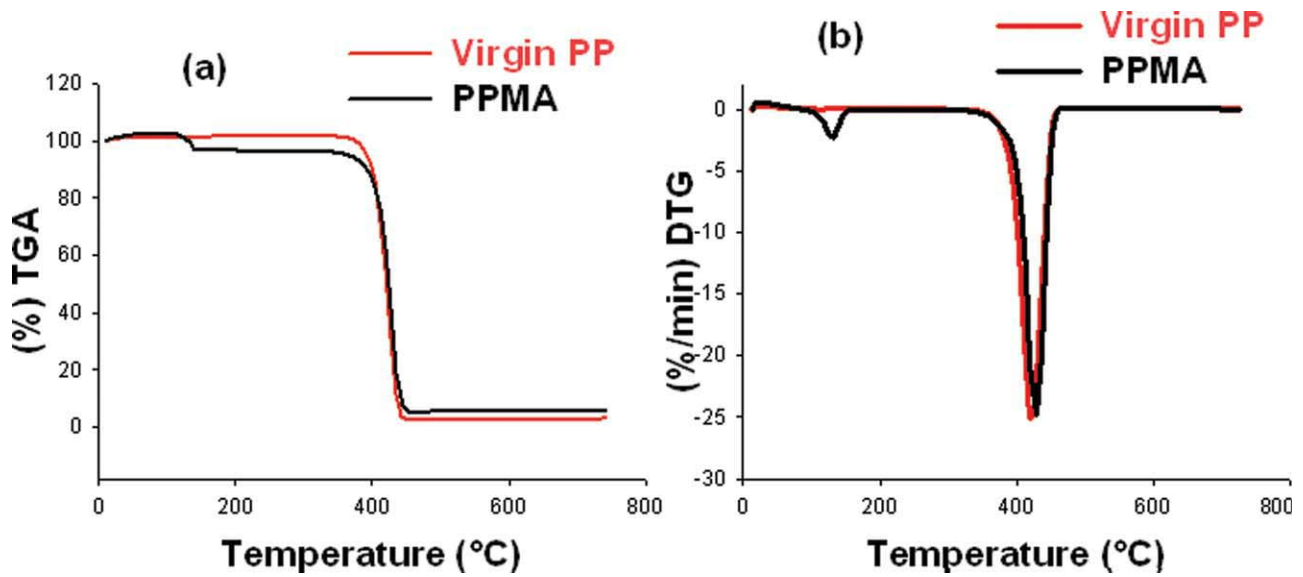

Figure 4 TGA–DTA thermograms of virgin PP and PPMA. (a) TGA curves, (b) DTG curves. [Color figure can be viewed in the online issue, which is available at wileyonlinelibrary.com].

observe that the composites treated by PPMA reveal higher rates of crystallinity than the other composites (composites untreated and composites treated by the VTAS).

Rheological studies: MFI

The evolution of the MFI according to the rate of the OHF untreated and treated is represented in Figure 6. According to these histograms, we perceive clearly that the MFI increase, as the rate of OHF increases, the MFI increases too. the similar results were found by Bledzki,[26] these results were attributed, on the one hand, on the thermo-oxidative decomposition of polypropylene during the preparation of the premixings of composite in the screw of

$$P_n \rightarrow R_r^{\bullet} + R_{n-r}^{\bullet}$$

$$P_n + R_r^{\bullet} \rightarrow P_n^{\bullet} + R_r H$$

$$P_n + R_{n-r}^{\bullet} \rightarrow P_n^{\bullet} + R_{(n-r)} H$$

Scission of chains (β-scission)

$$P_n^{\bullet} \rightarrow P_{n-r} + R_r^{\bullet}$$

Termination

$$P_n + R_r^{\bullet} \rightarrow P_n^{\bullet} + RH$$

$$P_n^{\bullet} + R_r^{\bullet} \rightarrow P_i$$

$$R_r^{\bullet} + R_r^{\bullet} \rightarrow P_{i'}^{'}$$

$$P_n^{\bullet} + R_r^{\bullet} \rightarrow P_n + R_r$$

Scheme 3 Mechanism of the thermal degradation.

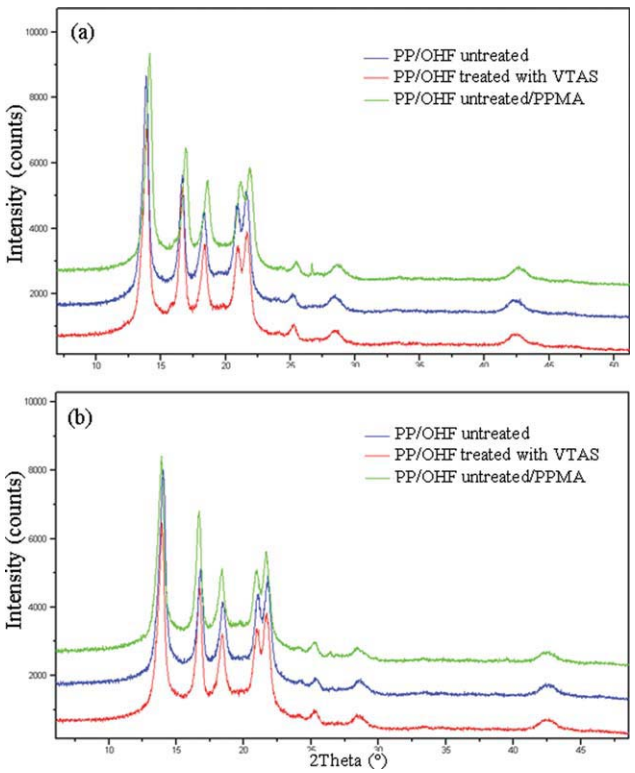

Figure 5 X-ray diffraction of the composites. (a) Formulation F10, (b) Formulation F20. [Color figure can be viewed in the online issue, which is available at wileyonlinelibrary.com].

TABLE II
Rate of Crystallinity of Composites

Samples	F0	F10N	F10S	F10P	F20N	F20S	F20P
Rate of crystallinity (%)	66	59	57	61	55	56	57

injection, but also with the high stress of shearing which induces the scissions of chains in the polypropylene, causing by the way the increase in MFI. Other share, the incorporation of a high rate of the OHF in the polypropylene increases the probability of the migration of a significant quantity of waxes on the surface leading to the increase in the capacity of flow of the composites by reducing the stress of friction between the past matter and the wall of the cylinder of the extruder. Moreover, the effect of the chemical treatment, we see clearly that the addition of PPMA and the VTAS reduce the MFI of the composites what is probably due to the improvement of interfacial adhesion between the OHF and the PP.

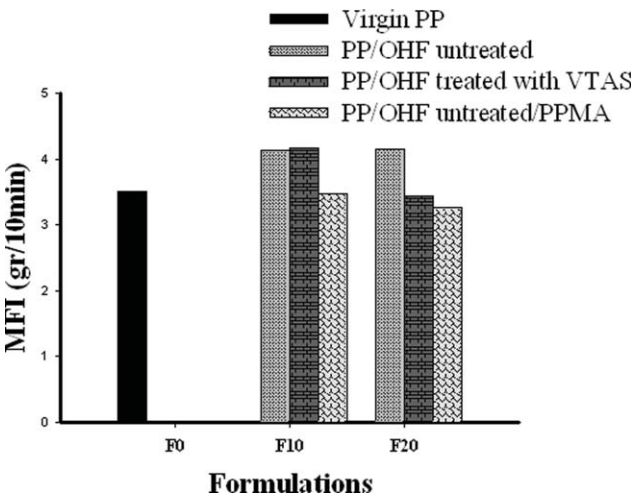

Figure 6 Evolution of the melt flow index according to the rate of the olive husk flour untreated and treated.

Water-absorption characteristics

This test enabled us to confirm the hydrophobic character of the matrix used. Indeed, the Figure 7 shows us clearly that the rate of WA of the PP does not exceed 0.04% whatever the time of immersion. It is evident in the figures that WA (%) increases with an increase in filler loading. With an increase in filler loading, the number of hydroxyl groups in the composites increases, which consequently increases the WA. We can also attribute this phenomenon to the bad interfacial adhesion between the PP and the OHF untreated resulting in the increase of microvoids. For example, samples F10*N*, F20*N* reached their water saturation with about 0.3%, 0.5%, respectively, at the end of 50 h of immersion. This background result confirmed by many research tasks such as Demir and Rahman.[16,27] However, the effect of the chemical treatment on the water-absorption behavior, we can notice that the composites treated with the VTAS and PPMA reveal a reduced WA compared with the untreated composites. This reduction is due to the reaction of the hydroxyls groups of fibers with the polar groups of the VTAS and PPMA by the means of the hydrogen bonds. Another reason can be explained by the improvement of interfacial adhesion led to considerable reduction in the vacuum, According to the Figure 7, we notices clearly that the composites treated by

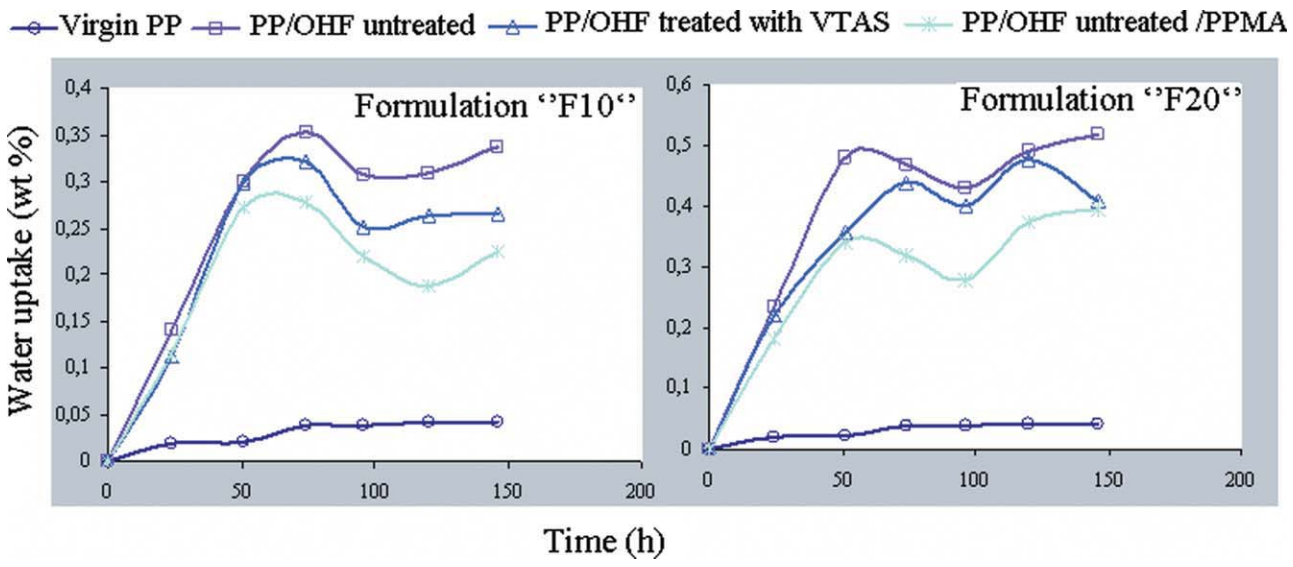

Figure 7 Water-absorption behavior. (a) Formulation F10, (b) Formulation F20. [Color figure can be viewed in the online issue, which is available at wileyonlinelibrary.com].

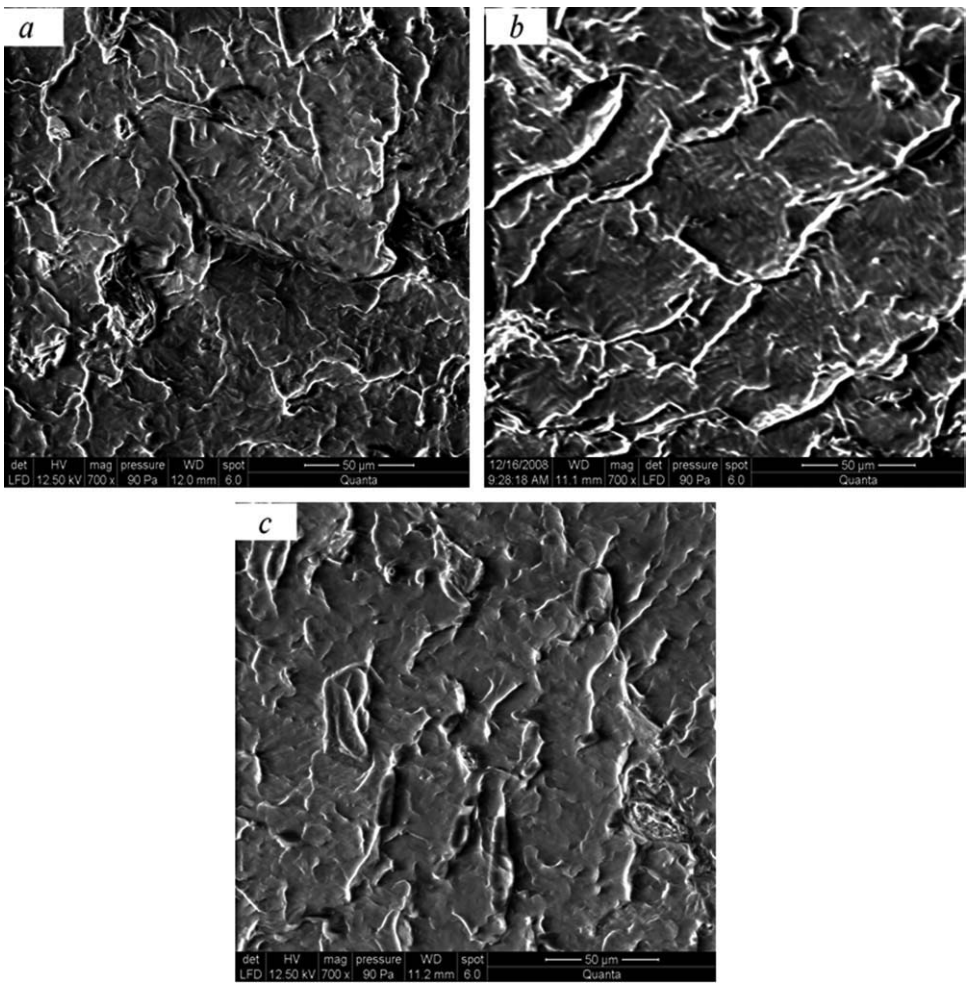

Figure 8 Scanning electron micrographs of fractured surface of PP/OHF composite loading at the 10 wt %: (a) composite untreated, (b) composite treated with silane, and (c) composite treated with PPMA.

PPMA reveal better results in the water-absorption behavior compared with the composites treated by the VTAS.

Scanning electron microscopy

The samples of the composites (treated and untreated) were analyzed by SEM to determine the morphological changes experienced by the flour as an effect on the treatment. Figure 8 illustrates a micrographs for the composites loading at 10% (w/w), (a) composites untreated, (b) composites treated with silane, (c) composites treated with PPMA.

For the composites untreated, we can see, the presence of many voids and cavities in the surface, indicating that the particles of OHF are pulled out from the matrix during fracture. This is attributed on the formation of the aggregates in the matrix. The formation of these aggregates affect negatively on a dispersion of the OHF in the matrix. On the other hand, the composites treated surface is smoother than those of composites untreated. We can be explained this by the better dispersion of flour and the treatment improved the adhesion between OHF and PP matrix.

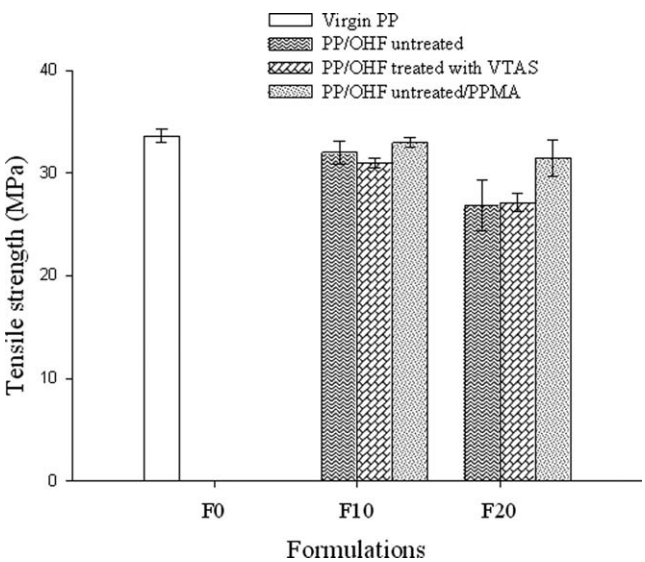

Figure 9 Tensile strength behavior.

Tensile strength

The tensile strength of different composites has been measured and the results are shown in Figure 9. As expected with increase in the filler loading in polymer matrix, PP-OHF composite showed a common phenomenon as shown by reduction of force at break for composites treated or untreated compared with virgin polypropylene matrix. Indeed, we can notice a decrease of a tensile strength with about 4.88%, 20.19% for the formulations prepared with the OHF untreated (F10*N*, F20*N*) compared with the virgin polypropylene, much research has confirmed this result as, Sonia, Demir, and Khalid.[7,16,28] This decrease can be attributed to poor dispersion of the flour in the matrix by forming aggregates which lead to the poor interaction between the OHF and the PP to cause an interruption in stress transferring along the applied force. Above all, lack of significant interfacial interaction between fillers and polymer matrix intensified the problem. They were not generally able to support stress transferred from the polymer and thus weakened the composite material. According to these histograms, we see a slight improvement of the tensile strength for the composites treated with the PPMA and VTAS compared with untreated composites. This increase is probably due to better dispersion of the OHF and particularly the reinforcement of interfacial bonds between the PP and OHF. We also noticed that the composites treated with the PPMA (F10 and F20) showed higher tensile strength compared with those treated with the VTAS. This can be explained by the ability of PPMA to form strong interfacial bonds between the PP and the OHF and thus a better transfer of constraint between the two phases compared with VTAS.

Young's modulus

The Figure 10 represents the evolution of Young's modulus according to the OHF loading. We see that the Young's modulus increases as OHF untreated increase. This increase in the Young's modulus indicates the rigidity of the composite increased, such results was confirmed by Metin and Dobircau.[6,29] Chemical treatment of the OHF led to the decrease of Young's modulus which probably caused greater adhesion interfacial OHF–PP composites compared with untreated.[16]

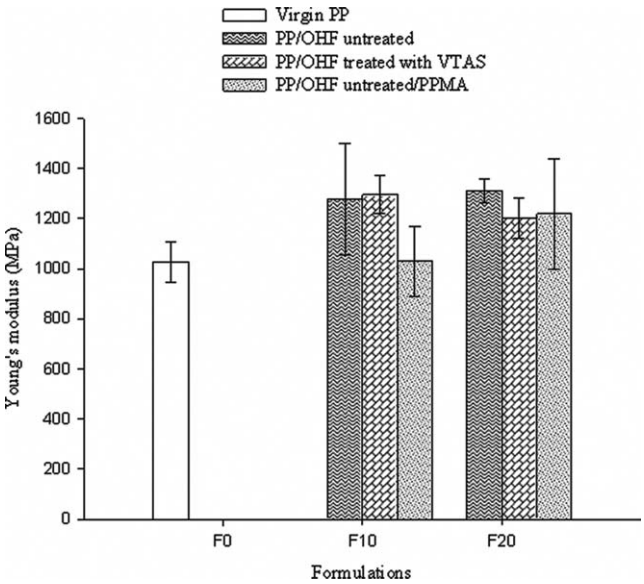

Figure 10 Young' modulus behavior.

Thermogravimetric analysis

Thermal stability of composite polymer fibers is a very important parameter for selecting the processing of these materials is their use. The manufacture of such materials is performed at elevated temperatures. Thus, the degradation of lignocellulosic fibers may occur during their transformations. For this purpose, composite materials that we prepared were subjected to thermal analysis (TGA–DTG). This analysis aims to determine the effect of chemical treatment of the OHF with a VTAS and PPMA (5% by weight) on the thermal properties of composites. According to the TGA thermogram represented Figure 11, we see clearly that the profiles of thermal degradation of composites are similar. The PP weight loss occurred in a one-step degradation process from 305 to 424°C. This result was confirmed by the presence of only one peak in derivative thermogravimetric curve (DTGmax) temperature at 394.4°C. However, the thermal degradation of OHF filled PP composites occurred in a three step degradation process, as also confirmed by the presence of three peaks for DTG curves. The first thermal degradation step may have corresponded to the hemicellulose localized in a temperature range of 232–308°C, the second is located at 308–350°C attributed to the degradation of cellulose, whereas the third stage is the degradation of the polymer (PP) and the lignin that is located between 350 and 454°C. In the addition, the incorporation of the OHFUT in polypropene led to a decrease in the temperature at the beginning of the decomposition and this decrease is even greater as OHF loading increase, it is in the round of 305.7°C for the PP and at 304.7°C, 275.6°C for formulations F10*N*, F20*N*, respectively. The decrease of the temperature at the beginning of the decomposition is probably caused by the decomposition of the components of the OHF. In the curves fo TGA–DTG of the composites we can see clearly that the composite modified by the PPMA reveal the

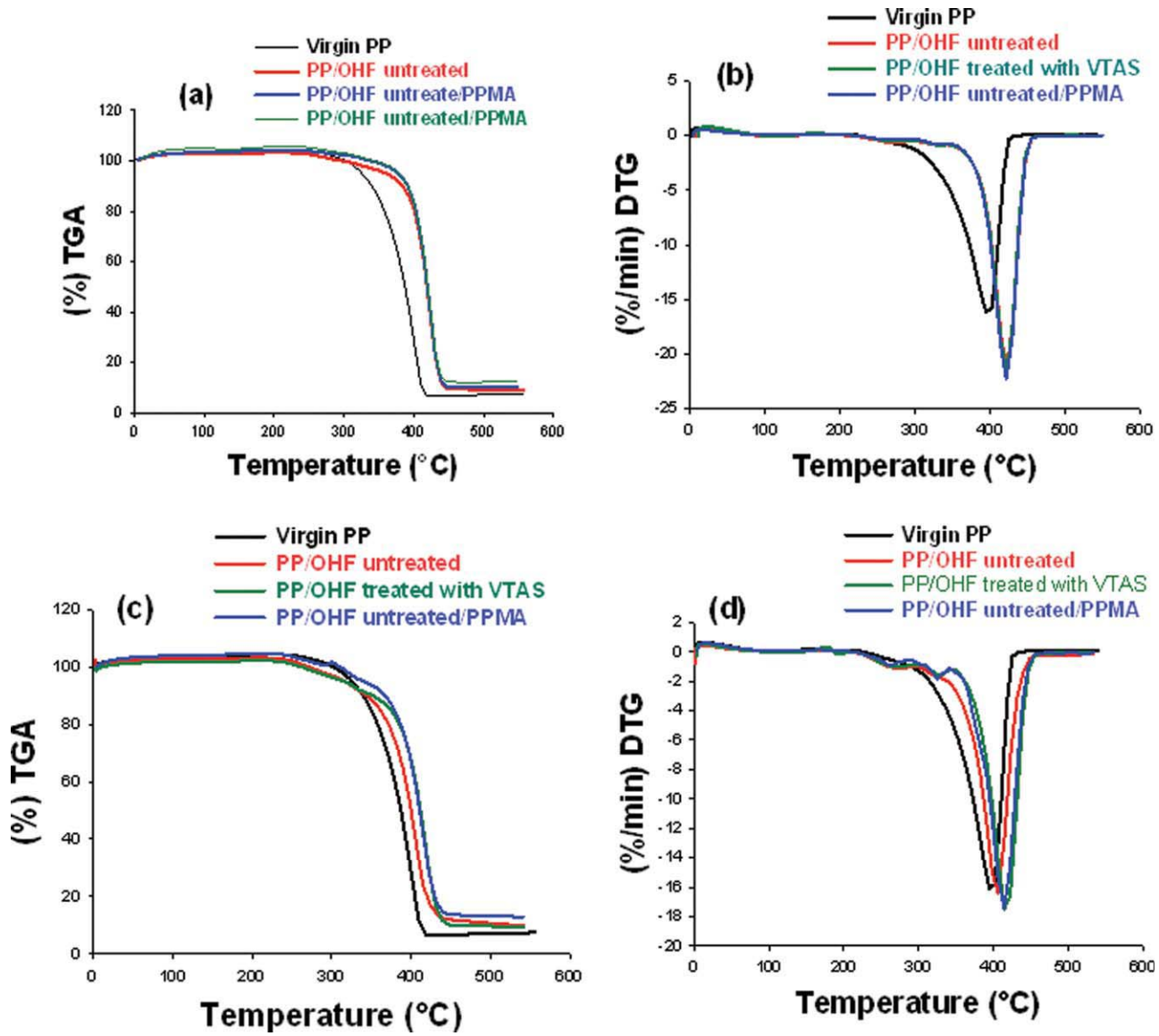

Figure 11 Thermal degradation behavior of the composites. (a) TGA curves of the formulation F10, (b) DTG curves of the formulation F10, (c) TGA curves of the formulation F20, (d) DTG curves of the formulation F20. [Color figure can be viewed in the online issue, which is available at wileyonlinelibrary.com].

better thermal stability compared with the composites modified by the VTAS and untreated composites. The thermal degradation of polypropylene stops at 460°C and it forms a dry residue of 7.5%. Conversely, then this temperature (460°C), samples prepared composites continue to undergo slow decomposition. It may also indicate that for the same loading rate composites are modified residue levels higher than nonmodified. Moreover, we can observe that the composites modified by the VTAS give residue levels higher than those modified by the PPMA and untreated. This can be explained by the presence of silica in the molecular structure of the OHFT which has a mineral character, according to the results of Aboulkas.[30]

CONCLUSIONS

The results of spectroscopy FTIR of PPMA reveal that the grafting reaction of AM on the PP is confirmed by the appearance of the absorption bonds at 1785 and 1708 cm^{-1} characteristic with the carbonyl groups (C=O) in the spectrum of PPMA. In addition, the absence of the absorption bond to 1600–1500 cm^{-1}, characteristic of the double bonds confirmed amply the grafting of AM on the PP. Moreover, the result of the FTIR of the OHF showed that the absorbance characteristics of the OHF decreases after treatment, which was attributed to the substitution of the hydroxyls groups by the silanols groups. This result was also confirmed by the test of water-absorption behavior of the composites. Indeed, we observed that the rate of WA of the composites

treated is lower than those of the composites untreated. Moreover, appearance of the absorption bonds in the rounding of 950 and 1195 cm^{-1} attributed to the asymmetrical vibrations of the bonds Si—O—Si and Si—O—CH3 is a signature of the reaction of silanization.

We also studied the mechanical behavior of composites PP/OHF. The results show that the mechanical properties (tensile strength, elongation at break, and impact resistance) decrease as the OHF untreated increase, this is attributed to the bad dispersion of the flour in the matrix, thus forming aggregates which lead to a weakened composite material.

We also noticed that the composites treated by PPMA (F10 and F20) have better tensile strength compared with those treated by the VTAS. This can be explained by the capacity of PPMA to form strong interfacial adhesion between the PP and the OHF and consequently a better transfer of stress between the two phases.

In conclusion, the two chemical treatments contribute to the improvement the interfacial properties PP/OHF. That results in obtaining better mechanical properties (more significant Young's modulus). On the other hand, elongation at break undergoes a clear reduction some is the load factor and the nature of the treatment.

The incorporation of the treated and untreated OHF improves the thermal stability of the composites. However, the use of the compatibilizer agent PPMA leads to a better thermal stability compared with the treatment of the OHF by the VTAS and the OHFUT.

References

1. Wulin, Q.; Takashi, E.; Takahiro, H. Eur Polym J 2006, 42, 1059.
2. Choi, Y. K. Doctoral thesis, Lyon, 2006.
3. Zita, D.; Livia, D.; Bela, P. Compos Part A 2007, 38, 1893.
4. Espert, A.; Vilaplana, F.; Karlsoon, S. Composites Part A 2004, 35, 1267–1276.
5. Maya, J. J.; Rajesh, D. A. Polym Compos, 2008.
6. Metin, D.; Tihminliog, F.; Balkose, D.; Ulku, S. Compos Part A 2004, 35, 23.
7. Sonia, M. B. N.; Graziela, S. C.; Simone, M. L. R. Polym Test 2007, 26, 619.
8. Bengtsson, M.; Oksman, K. Compos A 2006, 37, 752.
9. Corrales, F.; Vilaseca, F.; Llop, M.; Girones, J.; Mendez, J. A.; Mutje, P. J Hazard Mater 2007, 144, 730.
10. Kaci, M.; Djidjelli, H.; Boukerrou, A.; Zaidi, L. Exp Polym Lett 2007, 11, 467.
11. Derriche, R.; Berrahmoune, K. S. J Food Eng 2007, 78, 1149.
12. Pütün, A. E.; Uzun, B. B.; Apaydin, E.; Pütün, E. Fuel Process Technol 2005, 87, 25.
13. Djidjelli, H.; Benachour, D.; Boukerrou, A.; Zefouni, O.; Martinez-Véga, J.; Farenc, J.; Kaci, M. Exp Polym Lett 2007, 1, 846.
14. Garcia Martinez, J. M. J Polym Sci 1998, 483.
15. Nah, C.; Hong, C. K.; Hwang, I.; Kim, N.; Park, D. H.; Hwang, B. S. J Ind Eng Chem 2008, 14, 71.
16. Demir, H.; Atikler, U.; Balkose, D.; Thmnloglu, F. Compos Part A 2006, 37, 447.
17. Abdelmouleh, M.; Boufi, S.; Belgacem, M. N.; Dufresne, A. Compos Sci Technol 2007, 67, 1627.
18. Wang, W. Handbook of Polymers in Drug Delivery, Polymer Characterization Techniques; Taylor & Francis Group, LLC, 2006.
19. Pracella, M.; Chionna, D.; Anguillesi, I.; Kulinski, Z.; Piorkowska, E. Compos Sci Technol 2006, 66, 2218.
20. Mader, E.; Doan, T. T. L.; Brodowsky, H. Compos Sci Technol 2007, 67, 2707.
21. Fung, K. L.; Xing, X. S.; Li, R. K. Y.; Tjong, S. C.; Mai, Y. W. Compos Sci Technol 2003, 63, 1255.
22. Kim, H. S.; Lee, B. H.; Choi, S. W.; Kim, S.; Kim, H. J. Compos Part A 2007, 38, 1473.
23. Turmanova, SCh.; Genieva, S. D.; Exp Polym Lett 2008, 133.
24. Lin, K. Y.; Xanthos, M.; Sirkar, K. K. J Membr Sci 2009, 330, 267.
25. Jiang, X. L.; Sun, K.; Zhang, Y. X. Exp Polym Lett 2007, 283.
26. Bledzki, A. K.; Letman, M.; Viksne, A.; Rence, L. Compos Part A 2005, 36, 789.
27. Rahman, Md. R.; Huque, Md. M.; Islam, Md. N.; Mahbub, H. Compos Part A 2009, 40, 511.
28. Khalid, M.; Ratnam, C. T.; Chuah, T. G.; Salmiaton, A.; Thomas, S. Y. C. Mater Design 2008, 29, 173.
29. Dobircau, L.; Sreekumar, P. A.; Saiah, R.; Leblanc, N.; Terrié, C.; Gattin, R.; Saiter, J. M. Compos Part A 2009, 40, 329.
30. Aboulkas, A.; El harfi, K.; El bouadili, A. Fuel Process Technol 2009, 5, 722–726.